

A Comparison of Structure and Stability between the Group 11 Halide Tetramers M_4X_4 ($M = \text{Cu, Ag, or Au; } X = \text{F, Cl, Br, or I}$) and the Group 11 Chloride and Bromide Phosphanes $(XMPH_3)_4$

Peter Schwerdtfeger,^{*†} Robert P. Krawczyk,[†] Anton Hammerl,[‡] and Reuben Brown[§]

Institute of Fundamental Sciences, Massey University (Albany Campus), Private Bag 102904, North Shore MSC, Auckland, New Zealand, Department of Chemistry, Ludwig-Maximilians University of Munich, Butenandtstrasse 5-13 (Haus D), D-81377 Munich, Germany, and Department of Chemistry, University of Auckland, Private Bag 92019, Auckland, New Zealand

Received June 3, 2004

The tetramers of the group 11 (I) halides, M_4X_4 ($M = \text{Cu, Ag, or Au; } X = \text{F, Cl, Br, or I}$), and corresponding group 11 (I) phosphanes, chloride and bromide $(XMPH_3)_4$ ($X = \text{Cl or Br}$), are investigated by the density functional theory. All coinage metal(I) halide tetramers adopt squarelike ring structures with an out-of-plane distorted (butterfly) D_{2d} symmetry. These structures are much lower in energy than the more compact cubelike T_d arrangements, which maximize dipole–dipole interactions and more closely resemble the solid-state structures of the copper and silver halides. Phosphine coordination completely changes the structures of these M_4X_4 clusters. The copper(I) and silver(I) phosphane chloride and bromide tetramers adopt a heterocubane structure, slightly preferred over a step (ladder-type)-cluster structure well-known in the coordination chemistry of such compounds. In stark contrast, gold(I) phosphane chloride and bromide tetramers prefer assemblies of linear $XAuPH_3$ units with direct gold–gold contacts, resulting in a square planar, centered trigonal planar, or tetrahedral gold core.

Introduction

All group 11 elements in the oxidation state +I show a well-known tendency to form clusters, which often have short metal–metal bonds.¹ For gold compounds, these d^{10} – d^{10} closed-shell interactions² can be as large as 7–12 kcal/mol.^{3,4} In the coordination compounds of silver and copper, metal–metal interactions can also be present but are much less pronounced, with a reported maximum of only 4 kcal/mol for copper(I) compounds.⁵ These metallophilic interactions⁶ are due to a combination of correlation and relativistic

effects⁷ with added ionic contributions.⁸ Relativistic effects are also responsible for changing the coordination chemistry of gold compared to silver or copper. Clusters of coordinated copper(I) and silver(I) halides form structures mainly due to electrostatic contributions, such as dipole–dipole interactions, while gold prefers short gold–gold contacts between linear $X-Au-Y$ units. We note, however, that the special role of gold in such interactions has been questioned only very recently, where silver was found to produce larger metallophilic interactions compared to gold for the model compound $[\text{Cl}-M-\text{PH}_3]_2$ when high-level electron correlation was used.⁹

The existence of oligomers in the vapor over group 11 halide melts has long been recognized.^{10–12} Infrared,¹³ mass spectrometric,¹⁴ and photoelectronic¹⁵ studies of the vapors of cuprous chloride gave conclusive evidence of the presence of oligomeric molecules up to the pentamer, with the trimer

* Author to whom correspondence should be addressed. E-mail: p.a.schwerdtfeger@massey.ac.nz.

[†] Massey University.

[‡] Ludwig-Maximilians University of Munich.

[§] University of Auckland.

(1) Jansen, M. *Angew. Chem., Int. Ed. Engl.* **1987**, *26*, 1098.

(2) Hoffmann, R. *Angew. Chem.* **1982**, *94*, 725; *Angew. Chem., Int. Ed. Engl.* **1982**, *21*, 711.

(3) Schmidbaur, H. *Chem. Soc. Rev.* **1995**, *39*. (b) Pyykkö, P. *Angew. Chem., Int. Ed.* **2002**, *41*, 3573.

(4) Pyykkö, P. *Chem. Rev.* **1997**, *97*, 597.

(5) Hermann, H. L.; Boche, G.; Schwerdtfeger, P. *Chem.—Eur. J.* **2001**, *7*, 5333.

(6) Schmidbaur, H. *Gold Bull.* **2000**, *33*, 3.

(7) Pyykkö, P.; Tamm, T. *Organometallics* **1998**, *17*, 4842.

(8) Runeberg, N.; Schütz, M.; Werner, H.-J. *J. Chem. Phys.* **1999**, *110*, 7210.

(9) O'Grady, E.; Kaltsoyannis, N. *Phys. Chem. Chem. Phys.* **2004**, *6*, 680.

(10) Meyer, V.; Meyer, C. *Chem. Ber.* **1879**, *12*, 1112.

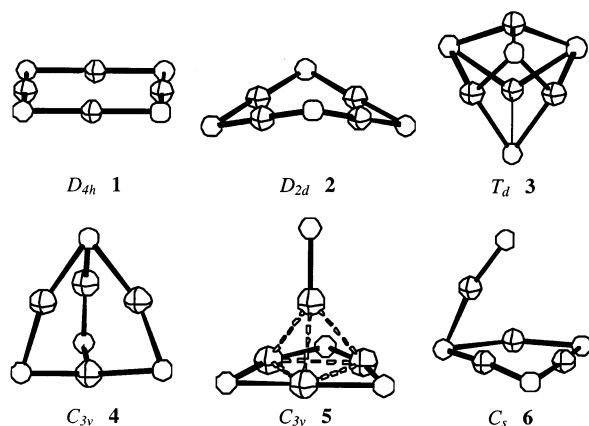


Figure 1. Minimum structures of coinage metal(I) halide tetramers, M_4X_4 , at the B3LYP level of theory.

and the tetramer being the predominant species under most conditions.¹⁶ Such metal–halide clusters are useful examples in the low-pressure CVD deposition for producing thin metal films.¹⁷ As far as the geometry of such clusters is concerned, $[CuCl]_4$ was originally predicted to have a tetrahedral symmetry.¹⁸ However, in a later study, the D_{4h} structure **1** was favored (Figure 1).¹⁹ Recent calculations for $[CuCl]_4$ support a ringlike D_{4h} minimum structure instead of a heterocubane T_d structure **3**, which is in agreement with the gas-phase electron diffraction experiments, with the T_d structure being 26 kcal/mol higher in energy.²⁰ In this study, the calculated IR spectrum is in good agreement with earlier measurements,²¹ and the gas electron diffraction also agrees with the D_{4h} structure.²⁰ There are a large number of experiments on group 11 halides which support oligomeric structures up to the hexamers in the gas phase. Calculations of the silver–bromide clusters, whose microcrystals play a crucial role in the photographic process,²² show that the

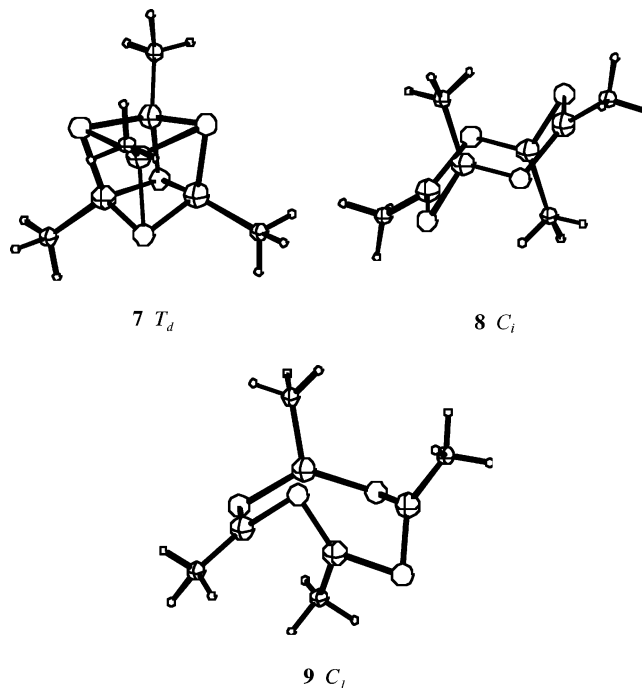


Figure 2. Heterocubane and step-cluster structures of tetrameric copper(I) and silver(I) phosphanes.

tetramers have a squarelike C_{2v} structure,²³ contrary to a previously predicted T_d minimum structure.^{24,25} A C_s structure **6** with an Ag_3Br_3 ring structure and a tetrahedral T_d structure were found to have higher energy. The $Ag_4(OH)_4$ cluster also has a planar cyclic structure.²⁶ Little is known about the structures of all other group 11 halide tetramers, and other possible arrangements, as shown in Figure 1, cannot be so easily excluded.

Coordination of electron-donating ligands, such as phosphane, to the group 11 metal halides completely changes the M_4X_4 structural units. In the solid state, the copper(I) and silver(I) halide phosphanes tend to oligomerize; for example, dimers²⁷ and two different tetrameric structures are observed.²⁸ One tetrameric structure represents the cubic M_4X_4 arrangement **7** and is found for many $[LMX]_4$ complexes of Cu(I) and Ag(I) ($X = Cl, Br, \text{ or } I$; $L = PPh_3, PEt_3, \text{ or } P(OPh)_3$) (Figure 2).²⁹ A previous theoretical study on copper(I) halide tetramers $Cu_4X_4L_4$ ($X = Cl, Br, \text{ or } I$; L

- (11) Binnewies, M.; Schaefer, H. Z. *Anorg. Allg. Chem.* **1972**, 395, 63. (b) Hilden, D. L.; Gregory, N. W. *J. Phys. Chem.* **1972**, 76, 1632. (c) Krabbes, G.; Oppermann, H. Z. *Anorg. Allg. Chem.* **1977**, 435, 33. (d) Polyachenok, L. D.; Nazarov, K.; Polyachenok, O. G. *Zh. Fiz. Khim.* **1977**, 51, 540.
- (12) Sugawara, K.; Wach, T.; Wanner, J.; Jakob, P. *J. Chem. Phys.* **1995**, 102, 544. (b) Hildenbrand, D. L.; Lau, K. H. *High Temp. Mater. Sci.* **1996**, 35, 11. (c) MacNaughton, R. M.; Bloor, J. E.; Sherrod, R. E.; Schweitzer, G. K. *J. Electron Spectrosc. Relat. Phenom.* **1981**, 11, 1. (d) Berkowitz, J.; Batson, C. H.; Goodman, G. L. *J. Chem. Phys.* **1980**, 72, 5829. (e) Kovacs, A.; Konings, R. J. M. *J. Mol. Struct.* **2002**, 643, 155.
- (13) Brewer, L.; Lofgren, N. *J. Am. Chem. Soc.* **1950**, 72, 3038. (b) Vanliere, M.; DeVore, T. C. *High Temp. Sci.* **1984**, 18, 185.
- (14) Guido, M.; Balducci, G.; Gigli, G.; Spoliti, M. *J. Chem. Phys.* **1971**, 55, 4566. (b) Wagner, L. C.; Robert, P.; Grindstaff, Q.; Grimley, R. T. *Int. J. Mass Spectrom. Ion Phys.* **1974**, 15, 255. (c) Guido, M.; Gigli, G.; Balducci, G. *J. Chem. Phys.* **1972**, 57, 3731. (d) Mao, D.; Liu, Z.; Li, R.; Qin, Q. *Huaxue Wuli Xuebao* **1996**, 9, 92. (e) Kudin, L. S.; Burdukovskaya, G. G.; Obukhova, T. S. *Izv. Vyssh. Uchebn. Zaved., Khim. Khim. Tekhnol.* **1992**, 35, 109.
- (15) Potts, A.; Lyus, M. L. *J. Electron Spectrosc. Relat. Phenom.* **1978**, 13, 305. (b) Koren, P. R.; Chen, F.; Davidson, E. R. *Mol. Phys.* **2001**, 99, 1329.
- (16) Locmelis, S.; Binnewies, M. Z. *Anorg. Allg. Chem.* **1999**, 625, 1578.
- (17) Bourhila, N.; Torres, J.; Palleau, J.; Bernard, C.; Madar, R. *Microelectron. Eng.* **1997**, 33, 25.
- (18) Wong, C. H.; Schomaker, W. *J. Phys. Chem.* **1957**, 61, 358.
- (19) Martin, T. P.; Schaber, H. *J. Chem. Phys.* **1980**, 73, 3541.
- (20) Hargittai, M.; Schwerdtfeger, P.; Balázs, R.; Brown, R. *Chem.—Eur. J.* **2003**, 9, 327.
- (21) Cesaro, S.; Coffari, E.; Spoliti, M. *Inorg. Chim. Acta* **1972**, 6, 513.

- (22) Fayet, P.; Granzer, F.; Hegenbart, G.; Moisar, E.; Pischel, B.; Woste, L. *Z. Phys. D: At., Mol. Clusters* **1986**, 3, 299.
- (23) Rabilloud, F.; Spiegelman, F.; L’Hermite, J. M.; Labastie, P. *J. Chem. Phys.* **2001**, 114, 289.
- (24) Srinivas, S.; Salian, U. A.; Jellinek, J. *Metal–Ligand Interactions in Chemistry, Physics and Biology*. In *NATO Science Series C: Mathematical and Physical Sciences*, Proceedings from the NATO Advanced Study Institute, Cetraro, Italy, Sept 1–12, 1998; Russo, N., Salahub, D. R., Eds.; Kluwer: Dordrecht, The Netherlands, 2000; Vol. 546, p 295.
- (25) Zhang, H.; Schelly, Z. A.; Marynick, D. S. *J. Phys. Chem.* **2000**, 104, 6287.
- (26) Bertolus, M.; Brenner, V.; Millie, P. *Eur. Phys. J.* **2000**, D11, 387.
- (27) Cassel, A. *Acta Crystallogr.* **1979**, B35, 174.
- (28) Hathaway, B. J. In *Comprehensive Coordination Chemistry*; Wilkinson, G., Gillard, R. G., McCleverty, J. A., Eds.; Pergamon Press: New York, 1987; Vol. 5, p 553.
- (29) Barron, P. F.; Dyason, J. C.; Engelhardt, L. M.; Healy, P. C.; White, A. H. *Inorg. Chem.* **1984**, 23, 3766. (b) Pike, R. D.; Starnes, W. H., Jr.; Carpenter, G. B. *Acta Crystallogr.* **1999**, C55, 162 and references therein.

= nitrogen organic base) also found cubelike structures.³⁰ The other possible arrangement is a step cluster, for example, a ladderlike (open-cube) structure **8** found for $[\text{XCu}(\text{PPh}_3)]_4$, with $\text{X} = \text{Br}$ or I .³¹ In the heterocubane structure, each metal atom has a formal coordination number of four. The distortion from an ideal cubic M_4X_4 core increases with the increasing size of the halogen ligand.²⁹ Sufficiently large phosphane ligands eventually stop the oligomerization process in copper and silver halides. For example, $\text{BrCuP}(\text{Mes})_3$ does not oligomerize; the molecule remains monomeric.³²

In distinct contrast, $\text{Cl}-\text{Au}-\text{PR}_3$ oligomerizes in the solid state by keeping the linear $\text{P}-\text{Au}-\text{Cl}$ structure intact and forming $\text{Au}-\text{Au}$ bonds.^{33,34} Phosphane ligands stabilize these aurophilic interactions, often inducing the formation of larger clusters.³⁵ The bulk of the phosphane ligand decides whether the compound stays monomeric,³⁶ dimerizes,³⁷ or polymerizes, forming chains.³⁸ Due to the preferred linear geometry of these gold coordination compounds, oligomerization only takes place with small phosphanes. It was also shown that in solution a facile ligand scrambling can occur between two LAuX molecules,³⁹ yielding a $[\text{LAuL}]^+[\text{XAuX}]^-$ salt. The energy difference for the ligand exchange in the solid state was shown to be very small.⁴⁰ This was confirmed by recent ab initio calculations.⁴¹

In this study, we investigate the structure and stability of all coinage metal(I) halide tetramers and the influence of phosphine coordination to the tetrameric group 11 chlorides and bromides. We investigate the bonding in these coordination compounds to see whether closed-shell interactions lead to the formation of metal-metal bonds. Computational Details are presented in the next section, followed by Results and Discussion. Conclusions are drawn in the last section.

Computational Details

All calculations were performed with Gaussian98⁴² using the density functional theory (DFT) with a B3LYP functional in combination with Los Alamos pseudopotentials and double- ζ

valence basis sets (LANL2DZ).⁴³ PH_3 was used as a model ligand for the phosphanes to reduce computational costs.⁶⁷ All minima were confirmed by frequency analyses. The tetrameric phosphane compounds have a very shallow potential surface regarding the rotation of the PH_3 units, especially for the silver compounds, and optimization with respect to PH_3 rotation leads to little energy change.

The D_{2d} and D_{4h} structures of the group 11 halide tetramers are very close in energy and were therefore optimized further using larger basis sets in connection with small-core Stuttgart pseudopotentials.⁴⁴ Here, we used the BPW91 functional because it gave

- (30) Vitale, M.; Ryu, C. K.; Palke, W. E.; Ford, P. C. *Inorg. Chem.* **1994**, *33*, 561.
 (31) Teo, B. K.; Calabrese, J. C. *Inorg. Chem.* **1976**, *15*, 2474 and references therein.
 (32) Alyea, E. C.; Ferguson, G.; Malito, J.; Ruhl, B. J. *Inorg. Chem.* **1985**, *24*, 3719.
 (33) Bott, R. C.; Bowmaker, G. A.; Buckley, R. W.; Healy, P. C.; Senake Perera, M. C. *Aust. J. Chem.* **1999**, *52*, 271.
 (34) Melnik, M.; Parish, R. V. *Coord. Chem. Rev.* **1986**, *70*, 157. (b) Gimeno, M. C.; Laguna, A. *Chem. Rev.* **1997**, *97*, 511. (c) Puddephatt, R. J. In *Comprehensive Coordination Chemistry*; Wilkinson, G., Gillard, R. G., McCleverty, J. A., Eds.; Pergamon Press: New York, 1987; Vol. 5, p 861.
 (35) Schwerdtfeger, P. *Angew. Chem., Int. Ed.* **2003**, *42*, 1892.
 (36) Baenziger, N. C.; Bennet, W. E.; Soboroff, D. M. *Acta Crystallogr.* **1976**, *B32*, 962.
 (37) Schmidbaur, H.; Weidenhiller, G.; Steigelmann, O.; Müller, G. *Chem. Ber.* **1990**, *123*, 285.
 (38) Angermeier, K.; Zeller, E.; Schmidbaur, H. *J. Organomet. Chem.* **1994**, *472*, 371.
 (39) Hormann-Arend, A. L.; Shaw, C. F. *Inorg. Chem.* **1990**, *29*, 4683.
 (40) Ahrland, S.; Dreisch, K.; Norén, B.; Oskarson, A. *Mater. Chem. Phys.* **1993**, *35*, 281. (b) Bauer, A.; Schmidbaur, H. *J. Am. Chem. Soc.* **1996**, *118*, 5324. (c) Schneider, W.; Bauer, A.; Schmidbaur, H. *J. Chem. Soc., Dalton Trans.* **1997**, 415.
 (41) Pyykkö, P.; Schneider, W.; Bauer, A.; Bayler, A.; Schmidbaur, H. *Chem. Commun.* **1997**, 1111.

- (42) Frisch, M. J.; Trucks, G. W.; Schlegel, H. B.; Scuseria, G. E.; Robb, M. A.; Cheeseman, J. R.; Zakrzewski, V. G.; Montgomery, J. A., Jr.; Stratmann, R. E.; Burant, J. C.; Dapprich, S.; Millam, J. M.; Daniels, A. D.; Kudin, K. N.; Strain, M. C.; Farkas, O.; Tomasi, J.; Barone, V.; Cossi, M.; Cammi, R.; Mennucci, B.; Pomelli, C.; Adamo, C.; Clifford, S.; Ochterski, J.; Petersson, G. A.; Ayala, P. Y.; Cui, Q.; Morokuma, K.; Malick, D. K.; Rabuck, A. D.; Raghavachari, K.; Foresman, J. B.; Cioslowski, J.; Ortiz, J. V.; Stefanov, B. B.; Liu, G.; Liashenko, A.; Piskorz, P.; Komaromi, I.; Gomperts, R.; Martin, R. L.; Fox, D. J.; Keith, T.; Al-Laham, M. A.; Peng, C. Y.; Nanayakkara, A.; Gonzalez, C.; Challacombe, M.; Gill, P. M. W.; Johnson, B.; Chen, W.; Wong, M. W.; Andres, J. L.; Gonzalez, C.; Head-Gordon, M.; Replogle, E. S.; Pople, J. A. *Gaussian 98*, revision A.9; Gaussian, Inc.: Pittsburgh, PA, 1998.
 (43) Hay, P. J.; Wadt, W. R. *J. Chem. Phys.* **1985**, *82*, 299.
 (44) Bergner, A.; Dolg, M.; Kuechle, W.; Stoll, H.; Preuss, H. *Mol. Phys.* **1993**, *80*, 1431.
 (45) Schwerdtfeger, P.; Brown, R.; Laerdahl, J. K.; Stoll, H. *J. Chem. Phys.* **2000**, *113*, 7110.
 (46) Schwerdtfeger, P.; Bowmaker, G. A. *J. Chem. Phys.* **1994**, *100*, 4487. (b) Andrae, D.; Häussermann, U.; Dolg, M.; Stoll, H. *Theor. Chim. Acta* **1990**, *77*, 123. (c) Dolg, M.; Stoll, H. *Theor. Chim. Acta* **1989**, *75*, 369.
 (47) Dunning, T. H., Jr. *J. Chem. Phys.* **1989**, *90*, 1007. (b) Woon, D. E.; Dunning, T. H., Jr. *J. Chem. Phys.* **1993**, *98*, 1358.
 (48) Schwerdtfeger, P.; Dolg, M.; Schwarz, W. H. E.; Bowmaker, G. A.; Boyd, P. D. W. *J. Chem. Phys.* **1989**, *91*, 1762.
 (49) Guichemerre, M.; Chambaud, G.; Stoll, H. *Chem. Phys.* **2002**, *280*, 71.
 (50) L'Hermite, J. M.; Rabilloud, F.; Labastie, P.; Spiegelman, F. *Eur. Phys. J. D: At., Mol. Opt. Phys.* **2001**, *16*, 77.
 (51) Reference deleted in proof.
 (52) Brown, J. R. A Theoretical Investigation of Group II Halides. Ph.D. Thesis, University of Auckland, Auckland, New Zealand, 2001.
 (53) Pyykkö, P.; Runeberg, N.; Mendizabal, F. *Chem.-Eur. J.* **1997**, *3*, 1451.
 (54) Rabilloud, F.; Spiegelman, F.; Heully, J. C. *J. Chem. Phys.* **1999**, *111*, 8925.
 (55) Pyykkö, P. *Chem. Rev.* **1988**, *88*, 563.
 (56) Schwerdtfeger, P.; Bruce, A. E.; Bruce, M. R. M. *J. Am. Chem. Soc.* **1998**, *120*, 6587.
 (57) Söhnel, T.; Hermann, H. L.; Schwerdtfeger, P. *Angew. Chem., Int. Ed.* **2001**, *40*, 4381.
 (58) Schwerdtfeger, P. *Chem. Phys. Lett.* **1991**, *183*, 457.
 (59) Schwerdtfeger, P.; McFeaters, J. S.; Liddell, M. J.; Hrusak, J.; Schwarz, H. *J. Chem. Phys.* **1995**, *103*, 245.
 (60) Bader, R. F. W. *Atoms in Molecules: A Quantum Theory*; Oxford University Press: Oxford, 1990. (b) Bader, R. F. W. *Chem. Rev.* **1991**, *91*, 893.
 (61) El-Bahraoui, J.; Dobado, J. A.; Molina, J. M. *J. Mol. Struct. (THEOCHEM)* **1999**, *493*, 249.
 (62) Bravo-Pérez, G.; Garzón, J. L.; Novaro, O. *Chem. Phys. Lett.* **1999**, *313*, 655.
 (63) Rabuck, A. D.; Scuseria, G. E. *Theor. Chem. Acc.* **2000**, *104*, 439. (b) Shapley, W. A.; Chong, D. P. *Int. J. Quantum Chem.* **2001**, *81*, 34.
 (64) Glass, G. E.; Konnert, J. H.; Miles, M. G.; Britton, D.; Tobias, R. S. *J. Am. Chem. Soc.* **1968**, *90*, 1131.
 (65) Adams, H. N.; Hiller, W.; Strähle, J. Z. *Anorg. Allg. Chem.* **1982**, *485*, 81. (b) Conzelmann, W.; Hiller, W.; Strähle, J.; Sheldrick, G. M. *Z. Anorg. Allg. Chem.* **1982**, *512*, 169. (c) Usón, R.; Laguna, A.; Jimenez, J.; Gomez, M. P.; Sainz, A.; Jones, G. P. *J. Chem. Soc., Dalton Trans.* **1990**, 3457.
 (66) Bauer, A.; Schmidbaur, H. *J. Am. Chem. Soc.* **1996**, *118*, 5324.
 (67) Häberlen, O. D.; Chung, S.-C.; Rösch, N. *Int. J. Quantum Chem.* **1994**, *28*, 595. (b) Häberlen, O.; Rösch, N. *J. Phys. Chem.* **1993**, *97*, 4970.

Table 1. Energies of the Coinage Metal(I) Halide Tetramers Relative to the Global Minimum Structure at the B3LYP/LANL2DZ Level of Theory (kcal/mol)

	1	2	3	4	5 ^a	6
CuF	0	0.2	41.7	37.1		36.2
CuCl	0.3 ^b	0	23.0	18.6		24.0
CuBr	0.2	0	16.7	13.3		18.7
CuI	1.2 ^b	0	10.6	8.7		12.5 ^b
AgF	0.6 ^c	0	12.9	24.5		28.9
AgCl	0	0.4	11.5	15.9		23.2
AgBr	0	0	11.1	13.0		<i>e</i>
AgI	0.1 ^b	0	10.8	10.4		<i>e</i>
AuF	0.6 ^b	0	82.7	47.8 ^b	39.7	37.5 ^b
AuCl	0	0.4	63.0 ^d	28.0	25.1	23.7
AuBr	0.1 ^b	0	57.9 ^d	24.4	21.5	24.4
AuI	0	0	55.9 ^d	21.2	18.6	17.8

^a Only for the gold halides. ^b TS leads to D_{2d} . ^c TS leads to D_{2h} . ^d TS leads to **5**. ^e TS leads to **4**.

more accurate results for the MX diatomics (M = Cu, Ag, or Au; X = F, Cl, Br, or I). The basis sets were altered by adding more diffuse and polarization functions to give the following contraction schemes: (3111111s/2211111p/311111d/111f) for Cu, (3111111s/3111111p/411111d/111f) for Ag, and (3111111s/2211111p/411111d/111f) for Au.^{45,46} For fluorine and chlorine, Dunning's⁴⁷ augmented triple- ζ basis sets were used with the f functions removed. For bromine and iodine, the Stuttgart basis set pseudopotential combinations⁴⁴ were altered to give (211111s/21111p/1d) and (211111s/111111p/1d) sets for Br and I, respectively.⁴⁶ For comparison, the tetramer of AuF was also optimized with a nonrelativistic pseudopotential.⁴⁸

The MX units have large dipole moments,⁴⁹ and the interaction in the cluster consists largely of dipole–dipole interactions. For the calculation of the influence of dipole interactions on the stability of the M_4X_4 clusters, a simple electrostatic model was adopted. To obtain the total energy, the dipole–dipole potential has to be augmented with a repulsive term between the atoms to avoid the collapse of the cluster from the purely attractive dipole–dipole interaction. A Lennard-Jones-type ($A r^{-12}$) repulsive term was therefore added at the ends of the dipole to give the final potential for the interaction between the two dipoles (in atomic units)

$$V(\boldsymbol{\mu}_1, \boldsymbol{\mu}_2) = \frac{\boldsymbol{\mu}_1 \boldsymbol{\mu}_2}{R^3} - \frac{(\boldsymbol{\mu}_1 \mathbf{R})(\boldsymbol{\mu}_2 \mathbf{R})}{R^5} + \sum_{i < j} \frac{A_{ij}}{r_{ij}^{12}} \quad (1)$$

R is the distance between the two dipoles (midpoint to midpoint), and r_{ij} is the distance between the atoms. We only use one parameter ($A = A_{ij}$) for all repulsive interactions such that the minimum of two parallel dipoles is at the unit length of $R_e = 1$ au ($A = 0.12403101$). The cluster geometry was optimized by numerical gradient techniques.

Results and Discussion

(MX)₄ Clusters. Figure 1 shows all of the structures found in the optimization procedure for the coinage metal(I) halide tetramers. Ring structures **1** and **2** have the lowest energy, in agreement with a number of theoretical studies for some metal halides (Table 1).^{20,50,51} Hence, the transition to a 3D solid-state-like structure does not yet occur for the tetramer, as pointed out previously by L'Hermite et al. for the case of silver bromide clusters.⁵⁰ Both structures **1** and **2** consist of squares with the halide atoms sitting at the corners and the metal atoms in the middle of the edges. The D_{2d} arrangement

2 is derived from the D_{4h} structure by folding the ring along a diagonal. The energy difference between these two structures is very small in all cases (0.4 kcal/mol or less at the B3LYP level of theory). Thus, the system behaves dynamically at room temperature, and gas-phase electron diffraction experiments may not be able to predict this symmetry breaking. Figure 3 shows a few different potential curves at the B3LYP level for the folding of the D_{4h} structure along the diagonal, which demonstrates that the potential energy surface describing the D_{4h}/D_{2d} distortion is quite shallow. Using the BPW91 functional with larger basis sets together with small-core Stuttgart pseudopotentials results in more-consistent geometries for the global minimum. Here, all clusters prefer the distorted D_{2d} structure except for the CuI tetramer, where the D_{2d} structure represents a first-order transition state with a weak distortion into D_2 symmetry, resulting in a planar rhombic Cu_4 core of local D_{2h} symmetry. As indicated in Table 2, the deviation from the ideal angle of 180° (D_{4h} symmetry), describing the distortion from D_{4h} to D_{2d} , increases with the decreasing electronegativity of the halide ligand.

The tetrahedral T_d structure **3**, which maximizes dipole–dipole interactions between the MX units forming a cube and, thus, resembles more closely the solid-state structure of the copper and silver halides, is between 10 and 20 kcal/mol higher in energy than the ring structures. This is in contrast to the finding of Zhang et al., who studied the $(AgBr)_n$ oligomers and proposed a tetrahedral structure for $(AgBr)_4$.²⁵ In their studies, the transition to 3D solid-state-like structures occurs from the tetramer onward. However, our findings are more in line with the recent studies of the silver bromide clusters by Rabilloud et al.,²³ who favor ringlike structures up to the hexamer. For the copper and gold fluoride tetramers, the tetrahedral arrangement is particularly disfavored (41.7 and 82.8 kcal/mol higher in energy, respectively). For the gold halides (apart from the fluoride), the tetrahedral structure represents a transition state leading to structure **5**. Structures **5** and **6** both have a $(MX)_3$ ring structure as a building block. The $(MX)_3$ ring is the global minimum structure for all of the coinage metal(I) halide trimers.^{20,52} In structure **5**, the gold end of the fourth MX molecule is above the $(MX)_3$ ring, thus forming a gold tetrahedron. In this case, an atom-in-molecule (AIM) analysis, according to Bader, clearly reveals gold–gold interactions. However, **5** is only a local minimum structure for the gold halide tetramers and does not represent a minimum for copper and silver, indicating the preference of gold for forming aurophilic interactions.⁴ For gold iodide, structure **5** is 21.2 kcal/mol higher in energy than the planar structure **1** and becomes less favored for the smaller halides. Thus, softer ligands lead to stronger aurophilic interactions, as pointed out before.⁵³ In **6**, a fourth MX molecule is connected to a halide in the corner of the $(MX)_3$ structure, forming a tail above the $(MX)_3$ ring structure. This structure is not particularly favored and often represents only a transition state leading to structure **5**. The C_{3v} structure **4** can be seen as a tetrahedron, consisting of the metal atoms with three

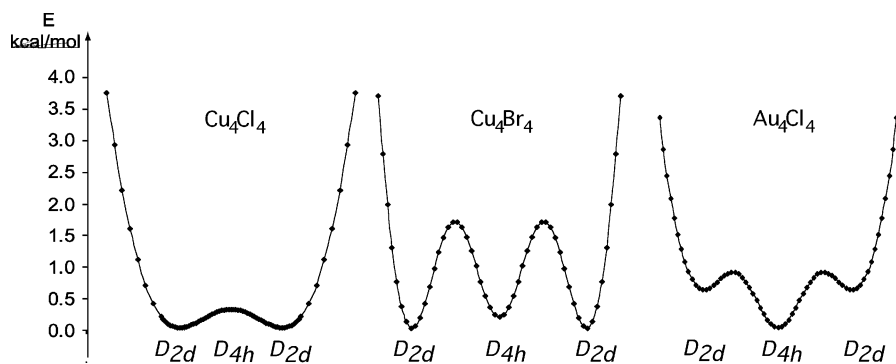


Figure 3. Three characteristic bending potentials (minimum energy paths) for the out-of-plane distortion from D_{4h} to D_{2d} for some selected molecules at the B3LYP/LANL2DZ level of theory. The x axis represents the out-of-plane distortion and can be obtained from the data shown in Table 2.

Table 2. Dissociation Energies D_n (kcal/mol) per Monomer Unit for the Process $M_4X_4 \rightarrow 4MX$ ($D_n = [E(MX) - E(M_nX_n)/n]$) of the Global Minimum Cu(I), Ag(I), and Au(I) Halide Structures Relative to the Monomers (the values include zero-point vibrational corrections) and Bonding Parameters (distances r in Å and angles α in deg; the shortest M–M distance is taken) Using the BPW91 Functional

	D_n	$r(M-X)_{\text{mon}}^a$	$r(M-X)$	$\Delta r(M-X)^b$	$r(M-M)$	$\alpha(M-X-M)$	$\tau(M-M-M-X)^c$	$\gamma(H-c-H)^d$
[CuF] ₄	42.3	1.750	1.861	0.111	2.548	86.4	169.3	158.2
[CuCl] ₄	42.6	2.052	2.155	0.103	2.594	74.0	148.3	113.5
[CuBr] ₄	40.5	2.176	2.286	0.110	2.575	68.6	142.9	101.6
[CuI] ₄ ^e	38.3	2.354	2.476	0.122	2.548	61.9	137.6	89.5
[AgF] ₄	32.2	1.983	2.091	0.108	2.977	90.8	169.0	158.0
[AgCl] ₄	33.1	2.281	2.360	0.079	3.093	81.9	157.4	133.0
[AgBr] ₄	32.4	2.393	2.490	0.097	3.015	74.5	144.6	106.9
[AgI] ₄	31.6	2.545	2.658	0.113	3.017	69.0	140.0	96.0
[AuF] ₄	34.7	1.956	2.079	0.123	2.937	89.9	162.9	146.5
[AuCl] ₄	37.4	2.234	2.331	0.097	3.162	85.4	157.4	134.2
[AuBr] ₄	36.4	2.357	2.452	0.095	3.179	80.8	151.6	118.4
[AuI] ₄	35.5	2.558	2.683	0.125	2.946	66.6	138.5	93.3

^a Bond distance of the monomer. ^b Difference between the M–X bond distances of the tetramer compared to the monomer. ^c Dihedral angle for the distortion into the D_{2d} structure (180.0° denotes the D_{4h} structure). ^d Folding angle (γ) of the butterfly structure; c denotes the center of the square if $\gamma = 180^\circ$ (i.e., the midpoint between the two top halogen (H) atoms). ^e D_{2d} structure taken for comparison, which is a first-order transition state. For more details, see the text.

chlorines attached to the edges and one face-centered. Structure **4** is in the same energy range as the tetrahedral structure **3**.

The dissociation energy per monomer unit is defined⁵⁴ as $D_n = [E(MX) - E(M_nX_n)/n]$ and decreases with the increasing size of the halide ligand (Table 2), except for the fluorides, which do not fit into this trend. Gold fluoride has the lowest binding energy of all gold halides. Perhaps more interesting is a comparison between the metals, which reveals that for a specific halide, copper has the highest binding energies, followed by gold and silver (Figure 4). This unusual trend is well-known for many properties of the group 11 compounds and is due to the relativistic effects of gold, which leads to a 6s orbital contraction/stabilization, giving Au approximately the same atomic size as Cu.⁵⁵ Indeed, non-relativistic calculations of the AuF tetramer give a reduced binding energy of 28.4 kcal/mol compared to 34.7 kcal/mol from calculations with a scalar relativistic pseudopotential (see discussions in refs 48 and 56). Although (AuF)₄ seems to be more stable than (AgF)₄, which is also the case for the predicted sublimation energies of the corresponding solid-state species,⁵⁷ we do know that solid AuF is not stable toward disproportionation into metallic gold and AuF₃, in contrast to silver(I) fluoride.

As one expects, the dipole interaction potential (eq 1) clearly prefers the cubic arrangement **3** over the ring structure **1**, in contrast to the DFT optimization. The ring structure is

therefore strongly stabilized by additional covalent (overlap) interactions. Figure 5 shows that the energy of ringlike structure **1** remains fairly independent of the magnitude of the dipole moment, whereas the cubic structure shows a strong dependence on the dipole moment. AgCl crystallizes in a (cubic) rock-salt structure, showing that with the addition of more MX units, the dipole interactions become more dominant. A change from the ring to the cubic structure is observed, but the exact cluster size for the transition between covalent and dipole structures has yet to be determined. Figure 5 demonstrates that large dipole moments will result in simple cubic ionic crystals, and the transition to the cubic structure may occur at an early stage in the cluster growth. For gold compounds, relativistic effects increase the electronegativity of gold⁵⁸ thus reducing the dipole moment for all gold halides (between 2 and 3 D),⁵⁷ and covalent interactions therefore become more important. Indeed, the crystal structures of the gold halides (AuCl, AuBr, and AuI) show rather unusual chainlike structures attributed to relativistic effects.⁵⁷

The metal halide bond distances get longer from the monomer to the tetramer.⁵² For most compounds, the difference is about 0.1 Å. In the nonrelativistic case, the Au–F bond length in Au₄F₄ is also considerably longer (2.228 Å) than that in the relativistic case (2.079 Å). This relativistic bond contraction of 0.15 Å is comparable to that of monomeric AuF, which is 0.17 Å.⁵⁹ In fact, the relativistic bond contraction for the gold halides can be clearly seen in

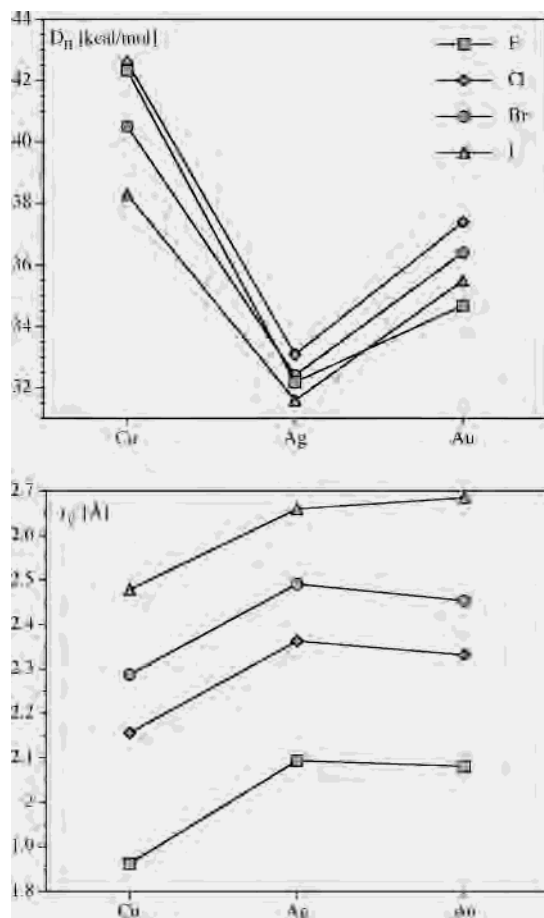


Figure 4. Dissociation energy per monomer unit and metal–halide bond distances for the group 11 halide tetramers.

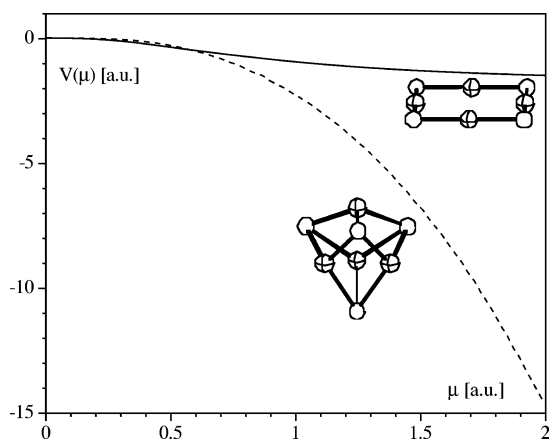


Figure 5. Total energy against the dipole moment for a dipole–dipole interaction, including a repulsive term as shown in eq 1. Ringlike structure (D_{4h} , solid line). Cubic structure (T_d , dashed line).

the changes in the trends of the group 11 halide tetramers (Figure 4). The Ag–Br bond distance (2.49 Å) and the MMMX angle (144.6°) of the AgBr tetramer are in reasonable agreement with the results (2.52 Å and 148°) obtained previously.²³ The Cu–Cl bond distance in the CuCl tetramer (2.155 Å) fits well with previous results from MP2 calculations (2.192 Å) and the experimental value (2.141 Å).²⁰ The metal–metal bond distances should get shorter with smaller halogen size. This is not always true. The change in structure from D_{4h} to D_{2d} causes an additional decrease in the metal–

Table 3. Mulliken Charges (q) and Orbital Populations at the Metal Center and the Orbitals of Metals and Halides in Tetramers with the BPW91 Functional

	q_M	q_M (mon) ^a	s_M	p_M	d_M	s_X	p_X
[CuF] ₄	0.50	0.51	0.34	0.41	9.72	2.01	5.49
[CuCl] ₄	0.09	0.35	0.65	0.49	9.75	1.94	5.09
[CuBr] ₄	0.10	0.31	0.60	0.45	9.83	1.86	5.19
[CuI] ₄ ^b	−0.12	0.12	0.83	0.41	9.86	1.89	4.97
[AgF] ₄	0.76	0.79	0.30	0.15	9.77	2.04	5.70
[AgCl] ₄	0.68	0.58	0.40	0.16	9.74	2.05	5.56
[AgBr] ₄	0.29	0.45	0.59	0.29	9.82	2.00	5.24
[AgI] ₄	0.30	0.39	0.54	0.33	9.82	2.03	5.21
[AuF] ₄	0.73	0.60	0.67	0.09	9.51	2.06	5.64
[AuCl] ₄	0.51	0.39	0.58	0.25	9.65	2.04	5.38
[AuBr] ₄	0.36	0.34	0.76	0.25	9.62	2.11	5.18
[AuI] ₄	0.09	0.26	0.79	0.34	9.78	2.15	4.95

^a Metal charge for the group 11 halide monomers. ^b D_{2d} structure taken for comparison, which is a first-order transition state. For more details, see the text.

metal distances; for example, we have a shortening of the Cu–Cu bond distance from 2.575 (Cu₄Br₄) to 2.548 Å (Cu₄I₄). As expected, the silver–silver bond distances are all larger than the Cu–Cu distances. The gold–gold bond distances have the same range as the silver–silver distances, which might indicate the presence of weak aurophilic interactions but also reflects the relativistic bond shortening. Using Bader’s atoms-in-molecules (AIM) approach,⁶⁰ no strong or weak bonds between the metal atoms of the gold halides in the D_{2d} and D_{4h} structures were detected. According to El-Bahraoui et al., the MX dimers (M = Cu or Ag; X = Cl, Br, or I) show metal–metal interactions;⁶¹ however, for both of the group 11 halide dimers and trimers, we cannot clearly identify such weak metal–metal interactions.⁵² As mentioned before, structure **5** clearly shows gold–gold interactions. Moreover, the D_{4h} to D_{2d} transition leading to a shortening of the metal–metal distances may be caused by such metallophilic interactions. The most likely case for strong aurophilic interactions would be Au₄I₄, with iodine being a rather soft ligand. We therefore discuss this molecule in more detail.

At the BPW91 level of theory, we obtain for Au₄I₄ a potential energy curve similar to that shown for Cu₄Br₄ in Figure 3, but with a slight modification. Here, the D_{4h} planar ring structure is a first-order transition state with $r_{Au-Au} = 3.713$ Å, $r_{Au-I} = 2.643$ Å, and an almost perfect right Au–I–Au angle of 89.2°. A number of stationary points were found on a very shallow potential hypersurface, including low-energy first- and second-order saddle points with energy differences to the global minimum of no more than 3 kcal/mol, which are not discussed here. A very small distortion ($\Delta E = -1.5$ kcal/mol; all ΔE values are with respect to the high-symmetry D_{4h} structure in the following) on that hypersurface leads to a local minimum of C_{2v} symmetry with one short ($r_{Au-Au} = 2.945$ Å) and one long ($r_{Au-Au} = 3.878$ Å) intrametallic distance. Here, the Au–I distances do not differ much ($r_{Au-I} = 2.649$ and 2.673 Å), and $\alpha_{Au-I-Au} = 66.9^\circ$. For this structure, the folding angle from the D_{4h} to the C_{2v} structure is $\gamma_{I-c-I} = 132.8^\circ$ (c denotes the center atom placed between the two top iodine atoms; see Table 3 for further explanations). The global minimum ($\Delta E = -2.6$

kcal/mol) has a rather short Au–Au bond distance of 2.946 Å and a slightly larger Au–I bond distance of 2.683 Å. For the angles, we have $\alpha_{\text{Au–I–Au}} = 66.6^\circ$ and $\gamma_{\text{I–c–I}} = 93.3^\circ$. This may indicate some aurophilic interactions. The energy differences are, however, very small. On the other hand, it is well-known that the density functional theory may not be able to correctly account for weak metallophilic closed-shell interactions. We therefore decided to carry out second-order many-body perturbation theory calculations for the electron correlation (MP2).

Because the MP2 calculations are more involved in terms of computer time, the Au (5s5p) and I (5s) orbitals were kept inactive in the MP2 procedure. The results are nevertheless interesting. The high-symmetry D_{4h} point remains a transition state, with the Au–Au bond distances substantially shortened (i.e., $r_{\text{Au–Au}} = 2.783$ Å, $r_{\text{Au–I}} = 2.651$ Å) and a rather large deviation from the ideal right Au–I–Au angle (58.3°). Hence, the structure is better described as a planar Au_4 cluster with four bridging iodine atoms. It was indeed found recently that the minimum structure of Au_4 is not tetrahedral, as one naively expects, but planar and of D_{2h} symmetry.⁶² The distorted Au_4I_4 D_{2d} minimum structure is now 6.6 kcal/mol lower in energy, significantly more than at the DFT level, clearly showing aurophilic interactions. Most surprising, however, is that the Au–Au bond distance slightly increases to 2.794 Å, while the Au–I bond distance decreases to 2.644 Å, compared to those of the D_{4h} structure. For the angles, we obtain $\alpha_{\text{Au–I–Au}} = 63.8^\circ$ and $\gamma_{\text{I–c–I}} = 81.8^\circ$. Hence, the distortion can be described as leaving the Au_4 cluster intact with two opposite bridging iodine atoms moving up and the other two iodine atoms moving down the plane. We point out, however, that more sophisticated electron correlation procedures, together with larger basis sets, are required to obtain a clearer picture of the bonding situation in these clusters since MP2 seems to overestimate such aurophilic interactions, as mentioned recently by O’Grady and Kaltsoyannis.⁹ We, therefore, did not reinvestigate the other M_4X_4 systems at the MP2 level of theory.

We finally mention Cu_4I_4 , where the D_{2d} structure is a first-order transition state in contrast to all of the other metal halide clusters. The distortion into D_2 symmetry gives the global minimum which is only 0.4 kcal/mol below the transition state. Here, the Cu_4 core is planar rhombic with a Cu–Cu bond distance of 2.518 Å and therefore shorter compared to that of the D_{2d} structure. The Cu–Cu–Cu angles (66.3 and 113.7°) deviate substantially from the ideal 90° angle. The Cu–I bond distances are 2.522 and 2.454 Å. Interestingly, the folding angle of $\gamma_{\text{I–c–I}} = 89.4^\circ$ does not change much from that of the ideal D_{2d} structure.

The reaction enthalpy for the formation of $[\text{CuCl}]_4$ was determined to be -168 kcal/mol,¹¹ agreeing well with our calculated value of -170 kcal/mol, considering that there is a deviation in the experimental values for the dimers and trimers¹⁴ and the general accuracy of generalized gradient or hybrid density functionals in combination with large basis sets.⁶³ We also mention that the MP2 dissociation energy for Au_4I_4 of 46.9 kcal/mol is significantly higher compared

Table 4. Energies (including zero-point correction in kcal/mol) of Cu(I) and Ag(I) Phosphane Halide Tetramers Relative to the Minimum Structure **7** at the B3LYP Level of Theory

	7	8	9
$[\text{ClCuPH}_3]_4$	0	11.8	
$[\text{BrCuPH}_3]_4$	0	11.1	10.9
$[\text{ClAgPH}_3]_4$	0	12.2	11.8
$[\text{BrAgPH}_3]_4$	0	9.9	9.6

to the DFT result shown in Table 3, and most of this difference can possibly be attributed to aurophilic interactions.

As far as the Mulliken analyses are concerned (Table 3), the most significant trends in the charges are due to the variation of the halides with large decreases in metal charges from F and I. As the transition to the tetramer from the monomer occurs, ligand-to-metal ($p_L \rightarrow s_M$) charge donation becomes more and more significant, with the p_M population becoming systematically larger for increasing cluster size. No significant metal–metal overlaps were found for the tetramers at the DFT level of theory, in line with the AIM analysis. The occupancy of the s orbitals increases from fluoride to iodide, with $[\text{CuI}]_4$ having a higher s occupancy ($s^{0.8}$) than the silver and gold compound (both $s^{0.5}$). While the d occupation increases from fluoride to iodide as expected, the differences are small. In the halides, the corelike s orbitals are fully occupied, and the p orbitals become less occupied from fluoride to iodide. Compared to the monomeric units, the metal s orbitals are more depopulated and, correspondingly, the d orbital occupation decreases. In summary, the MX bonds can best be described as ionic with a charge transfer from the metal s to the halide p orbitals. There is a smaller amount of π bonding due to the donation from the p ligand to the metal p_π orbitals, which is more pronounced in the tetramers and increases from F to I. Metal d participation in the bonding becomes more important for the softer ligands.

(XMPH₃)₄ Clusters. The coordination of phosphane completely changes the structures of these tetramers (Figures 2 and 6). The ring structure found for the halides does not represent a minimum on the potential energy surface. The copper and silver chloride and bromide phosphane tetramers have minima for a heterocubane T_d structure **7**, a C_i step-cluster structure **8**, and a C_1 structure that is a distortion of **8** (Table 4). For all copper and silver compounds, **7** represents the global minimum structure. Structure **9** is about 10 kcal/mol higher in energy, and **8** is about 0.3 kcal/mol higher in energy than **9**, except for $[\text{CuCl}(\text{PH}_3)]_4$, where **9** does not represent a minimum structure.

The gold chloride and bromide phosphane tetramers have different structures compared to the copper and silver homologues (Table 5). Structures **7–9** and planar ring structures, such as those found for the halide tetramers, do not represent minima for the gold compounds. Such ringlike structures are better known for Au(III) coordination compounds.⁶⁴ Unlike the copper and silver compounds, the X–Au–P unit remains linear in all cases. The interactions responsible for the aggregation are metal–metal interactions.⁶ With the exception of **11**, the gold compounds form dimers,

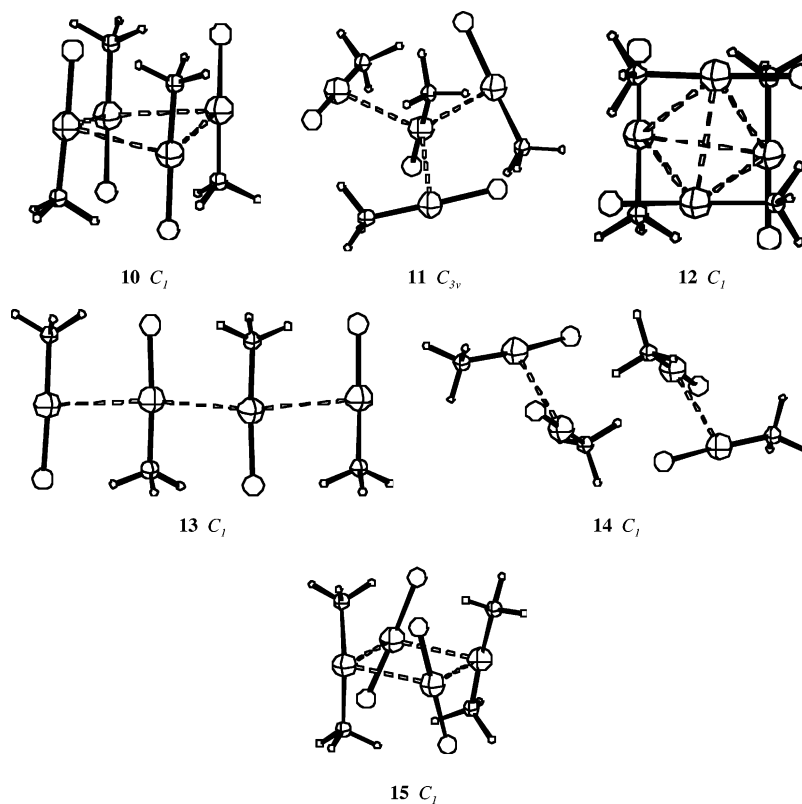


Figure 6. Computed structures of the gold(I) phosphane halide tetramers.

Table 5. Energies (including zero-point correction, in kcal/mol) for the Au(I) Phosphane Halides Relative to the Minimum Structure at the B3LYP Level of Theory

	10	11	12	13	14	15
[ClAuPH ₃] ₄	0	2.4	1.9	5.6	10.6	9.5
[BrAuPH ₃] ₄	0.3	0	1.2	4.1	8.7	8.9

which prefer an angle of about 30° between the X–Au–P units to a parallel arrangement. Combination of the dimers results in the observed structure types.

In **10**, four gold atoms are in a square planar arrangement with the halide and phosphane ligands alternating above and below the plane. In **11**, three XAuPH₃ molecules form a propeller around a central XAuPH₃ unit with three Au–Au interactions. Structure **12** shows two dimers stacked alternately, forming a Au₄ tetrahedron with two smaller and two longer gold–gold bonds. A linear structure **13** and two separate dimers **14** are 5 and 10 kcal/mol higher in energy than structures **10**–**12**. Due to the observed ligand exchange of some gold compounds to form [AuX₂][−][Au(PH₃)₂]⁺ complexes,³⁹ we optimized all previous structures, as well as those mentioned earlier,⁴¹ to determine the energetics of this ligand exchange. Only one ionic minimum structure was found. Structure **15** has a distorted square planar arrangement like **10**, with alternating AuX₂[−] and Au(PH₃)₂⁺ units. No minimum was found for the (+ − − +) or (− + + −) arrangements of LAuL⁺ and XAuX[−],⁴¹ which can be understood from simple electrostatic arguments. However, these structures do exist with ligands other than PR₃ or X = halogen, although they are rare, for example, in [AuX(py)]₄ (X = Cl, Br, or I; py = pyridine)⁶⁵ or more recently in (Me₂PhP)AuGeCl₃.⁶⁶ Structure **15** is ~10 kcal/mol higher

in energy for chloride and bromide than **10**–**12**. In the solid state, **15** might very well be favored over **10**–**12** because of additional ionic interactions with other units.

The binding energy for the copper and silver chloride phosphane tetramers, as defined for the pure halide tetramers, is ~18 kcal/mol. For the bromides, it is slightly lower at ~16 kcal/mol (Table 6). The gold tetramers show lower binding energies of 12.2 kcal/mol for the chloride and 9.9 kcal/mol for the bromide. The binding energies are much lower than those of the bare halide tetramers, showing that the monomeric phosphanes are electronically more saturated. The lower binding energy for the bromides compared to that of the chlorides follows the trend for the halide tetramers.

The M–X bond distances of the copper and silver compounds are about 0.35 Å longer in the tetramers than in the monomers due to the double coordination of the halides in the monomers. The M–P bond distances are only ~0.05 Å longer in the tetramers than in the monomers. In the gold tetramers, the M–X and the M–P bond lengths become only slightly (ca. 0.05 Å) longer. The bond distances of crystal structures are shorter than the calculated ones, especially for the M–P distances. We note that using PH₃ ligands instead of other PR₃ ligands can have a non-negligible influence on the bonding and stability of these phosphane complexes.⁶⁷

The metal–metal bond distances in the copper (3.247 Å for Cl and 3.111 Å for Br) and silver (3.622 Å for Cl and 3.623 Å for Br) phosphane halides are considerably longer than the metal–metal distances in the halides and indicate that there is no metal–metal interaction present. In [ClAuPH₃]₄ (**10**) we find one short Au–Au bond distance of 3.481 Å, another of 3.615 Å, and two long gold–gold

Table 6. Binding Energies (E_b) per Monomer Unit (kcal/mol) of the Global Minimum of Cu(I), Ag(I), and Au(I) Phosphane Halide Structures Relative to the Monomers and Bonding Parameters (distances r in Å and angles α in deg) with the B3LYP Functional

	ΔE_b	$r(\text{M}-\text{X})$	$r(\text{M}-\text{X})_{\text{mon}}$	$\Delta r(\text{M}-\text{X})$	$r(\text{M}-\text{X})_{\text{exp}}^a$	$r(\text{M}-\text{P})$	$r(\text{M}-\text{P})_{\text{mon}}$	$r(\text{M}-\text{P})_{\text{exp}}$	$r(\text{M}-\text{M})$	$\alpha(\text{P}-\text{M}-\text{X})$
[ClCuPH ₃] ₄	18.8	2.517	2.158	0.359	2.35–2.53	2.341	2.297	2.15	3.247	118.7
[BrCuPH ₃] ₄	16.9	2.647	2.297	0.350	2.49–2.75	2.374	2.309	2.15–2.17	3.111	113.3
[ClAgPH ₃] ₄	18.1	2.754	2.381	0.373	2.65	2.615	2.519	2.39	3.622	119.7
[BrAgPH ₃] ₄	15.6	2.883	2.509	0.374	2.74	2.615	2.535	2.41	3.623	117.1
[ClAuPH ₃] ₄	12.2	2.432	2.376	0.056		2.383	2.389		3.817 (2x) 3.615	178.3 179.9
[BrAuPH ₃] ₄	9.9	2.539 2.557	2.497	0.042		2.399 2.409	2.404		3.481 3.265	177.7 178.6 179.9

^a Distances from XCuP(OPH)₃ (ref 29b) and XAgPEt₃ (ref 69).

Table 7. Mulliken Charges of the Group 11 MX(PH₃) (X = Cl or Br) Monomers and Tetramers

	XMPH ₃			[MX(PH ₃) ₄]		
	M	X	P	M	X	P
[ClCuPH ₃] ₄	0.15	−0.37	0.01	0.14	−0.30	0.04
[BrCuPH ₃] ₄	0.13	−0.35	0.02	0.07	−0.24	0.04
[ClAgPH ₃] ₄	0.15	−0.37	0.16	0.21	−0.35	0.03
[BrAgPH ₃] ₄	0.13	−0.35	0.22	0.16	−0.31	0.02
[ClAuPH ₃] ₄	−0.04	−0.27	0.06	−0.09 to −0.11	−0.30 to −0.32	0.12 to 0.15
[BrAuPH ₃] ₄	−0.08	−0.22	0.05	0.06 −0.21 (3x)	−0.24 −0.26 (3x)	0.15 0.12 (3x)

distances of 3.817 Å. Despite the long bond distances for [ClAuPH₃]₄, structure **10** is 2.4 kcal/mol lower in energy than **11**, which has three shorter Au–Au bond interactions compared to the four longer interactions of **10**. The ClAuPH₃ dimer has two structures very close in energy, one with large gold–gold bond distances and close H–Cl interactions,⁶⁸ thus maximizing dipole–dipole interactions, and the other one with close gold–gold bond distances, thus maximizing aurophilic interactions. The second structure is slightly lower in energy. Structures **10** and **11** show the same pattern; in **10**, the hydrogen–chlorine close contacts are dominant, and in **11**, aurophilic interactions become important. For the bromide structure, the global minimum **11** is only 0.3 kcal/mol lower in energy than **10**. Here, the gold–gold bond distances to the central gold atom are 3.265 Å (between the peripheral gold atoms the distance is 5.646 Å) and the torsion angles close to 120° between two XAuPR₃ units, thus maximizing aurophilic interactions and minimizing dipole–dipole interactions. In comparison, for **10**, the minimum gold–gold bond distance is 3.638 Å. This has been discussed extensively in the past.^{4,8,68} We note that the density functional calculations will underestimate the dispersive type of interactions, and the calculated Au–Au bond distances are probably too large.

The metal and halide charges of the copper and silver XMPH₃ monomers are much lower than those of the corresponding halides due to the electron-donating character of the PH₃ ligand (Table 7). The charges of the copper and silver halide tetramers remain almost identical to those of the monomers. The electronegativity of gold is increased by relativistic effects,⁵⁸ and the metal charges for gold are negative in contrast to copper and silver. The propeller-like

bromide structure **11** has three gold charges of −0.21 and a positive charge of 0.06 on the central gold atom.

Conclusion

All group 11 metal halide tetramers adopt ringlike structures. [CuCl]₄ has already been explored in the D_{4h} ring structure, with the halogen atoms on the corners and the metal atoms in the middle of the edges. Our calculations indicate that all of the tetramers have D_{2d} structures, which are derived from the D_{4h} structure by folding the ring along a diagonal. Using the AIM method, no clear bond paths were found between the metal atoms in the group 11 halides at the DFT level of theory. However, at the MP2 level, aurophilic interactions were clearly identified for Au₄L₄. The very similar structures obtained for all group 11 halide clusters suggest that the well-known differences for the solid-state structures between the copper and silver halides on one hand (mostly cubic) and the gold halides on the other hand (chainlike structures caused by relativistic effects)⁵⁷ are not evident yet for such a small cluster size. The potential energy surface shows a number of local minima and transition states lying close, within a few kilocalories per mole. Different quantum theoretical methods may therefore yield different structures for the global minimum. Nevertheless, the system probably behaves dynamically at room temperature with fast interconversions between the minima, and gas-phase electron diffraction studies at such temperatures may not detect such distortions.

While all group 11 halide tetramers have ringlike structures, the phosphane complexes of the group 11 chlorides and bromides are not stable in this configuration. Due to a lower charge separation in the phosphanes, the binding energy per monomer unit is lower in the phosphane coordinated tetramers. The copper and silver halide phosphane tetramers favor heterocubane structures with about 10 kcal/mol over two slightly different step-cluster structures.

(68) Pyykkö, P.; Zhao, Y. *Angew. Chem., Int. Ed. Engl.* **1991**, *103*, 622; *Angew. Chem.* **1991**, *30*, 604.

(69) Churchill, M. R.; Donahue, J.; Rotella, F. J. *Inorg. Chem.* **1976**, *15*, 2752.

The gold tetramers have totally different structures since they retain their linearity upon oligomerization. Perhaps the explanation for the occurrence of aurophilic interactions may be found here as linear X–Au–Y units facilitate such interactions. $[\text{XAuPH}_3]_4$ bromides and chlorides show two different structure types, one governed by dipole–dipole interactions and the other by gold–gold interactions. Both structures are within 2 kcal/mol for both the chloride and bromide. The dipole structure is favored for the chloride, the other for the bromide. The minimum structure for the chloride is a Au_4 square with alternating substituents above and under the plane, and the bromide structure is best described as three molecules forming a propeller around the central hub.

The investigated copper and silver halide phosphanes have no significant metal–metal interactions at the DFT level of

theory. The metal–metal distances are too long, which is consistent with the ClCuPH_3 and BrAgPH_3 dimers, where no metal–metal bonds were found.⁶¹ The tetramers of the gold halide phosphanes show a variety of structures that are very close in energy and have different contributions from electrostatic interactions between the ligands plus close metal–metal contacts.

Acknowledgment. This work was supported by the Alexander von Humboldt Foundation and the Marsden Fund administered by the Royal Society of New Zealand. We are grateful to the Allan Wilson Centre for large amounts of computer time on their high-performance parallel computer HELIX.

IC0492744